

Molecular modelling approaches for the identification of potent sodium-glucose cotransporter 2 inhibitors from *Boerhavia diffusa* for the potential treatment of chronic kidney disease

Shanmugampillai Jeyarajaguru KABILAN ¹ , Oviya SIVAKUMAR ¹ , Selvaraj KUNJIAPPAN ¹ , Parasuraman PAVADAI ² , Krishnan SUNDAR ^{1*} 

¹ Department of Biotechnology, Kalasalingam Academy of Research and Education, Krishnankoil-626126, Tamilnadu, India.

² Department of Pharmaceutical Chemistry, Faculty of Pharmacy, M.S. Ramaiah University of Applied Sciences, Bengaluru-560054, Karnataka, India.

* Corresponding Author. E-mail: sundarkr@klu.ac.in (S.K.); Phone: +91- 9342772320.

Received: 6 August 2024 / Revised: 1 November 2024 / Accepted: 7 November 2024

ABSTRACT: Chronic Kidney Disease (CKD) is a major global health issue affecting 10–14% of the global population. The current study used molecular modelling tools to identify potential bioactive compounds from the folk medicinal plant, *Boerhavia diffusa* for the treatment of CKD. The target protein was identified as sodium/glucose co-transporter 2 (SGLT2), which has been linked to the development of CKD. Using IMPPAT database, twenty-five bioactive molecules from *B. diffusa* were identified and docked against the SGLT2 protein to determine their binding affinity. The molecular docking of the twenty-five compounds *B. diffusa* revealed that punarnavoside ($-10.2 \text{ kcal} \times \text{mol}^{-1}$), and flavone ($-9.3 \text{ kcal} \times \text{mol}^{-1}$) were potential drug candidates. Metabolites of punarnavoside were also predicted and re-docked with the same target. Among the metabolites, punarnavoside-1 exhibited a better docking score ($-10.3 \text{ kcal} \times \text{mol}^{-1}$). The pharmacokinetic and physico-chemical properties of the compounds were also predicted and assessed using web-based tools. Punarnavoside and flavone exhibited drug-like properties while having a lower toxicity profile. According to this study, the *in-silico* results of *B. diffusa* biomolecules were comparable to dapaglifozin, a standard CKD drug. As a result, punarnavoside and flavone are potent and safe SGLT2 inhibitors that could potentially be used in the treatment of CKD. Further experimental and clinical research is required to determine their efficacy and safety in the treatment of CKD.

KEYWORDS: Chronic kidney disease; *Boerhavia diffusa*; sodium/ glucose co-transporter 2; molecular modelling tools, SDG 3

1. INTRODUCTION

Kidney plays an essential role in human physiology because it removes waste from circulation, regulating electrolytes, and maintains body fluids. The kidney is also involved in hormone synthesis and vitamin A production, which controls red blood cell formation, and regulates blood pressure and calcium metabolism. Because of all these, kidney is involved in a complex interaction with other organs. Chronic kidney disease (CKD) refers to a group of diseases that affects the structure and function of the kidneys [1]. CKD affects the entire human body and is a global public health concern because it can lead to renal failure, cardiovascular disease (CVD), and premature death [2].

CKD is defined as kidney damage or glomerular filtration rate of less than 60 mL per min per 1.73 m² for at least three months [3]. Though people with CKD lose kidney function over time, they may be unaware of their condition until it is advanced. The glomerulus (the minuscule kidney units) is made up of glomerular endothelial cells (GECs), a glomerular basement membrane (GBM), podocytes, mesangial cells, and parietal epithelial cells. CKD destroys the podocytes in the Bowman's capsule of the kidneys, which wrap around the glomerulus capillaries and are unable to perform the selective permeability of the glomerular filtration barrier.

How to cite this article: Kabilan SJ, Sivakumar O, Kunjiappan S, Pavada P, Sundar K. Molecular modelling approaches for the identification of potent sodium-glucose cotransporter 2 inhibitors from *Boerhavia diffusa* for the potential treatment of chronic kidney disease. J Res Pharm. 2025; 29(5): 1851-1877.

Type 1 and type 2 diabetes, hypertension, glomerulonephritis, interstitial nephritis (inflammation of the tubules and surrounding structures of the kidney), vesicoureteral reflux (a condition that causes urine to back up into the kidneys), pyelonephritis, and prolonged obstruction of the urinary tract due to enlarged prostate, kidney stones and some tumors, polycystic kidney disease or other inherited kidney diseases are the most common primary causes of CKD in high- and middle-income nations [4].

CKD affects approximately 10% of the global population and was ranked 18th in the Global Burden of Disease survey [5]. The WHO estimates that treating end-stage CKD incurs significant financial burden in high-income countries, accounting for 2 to 3 % of their health care budget [6]. Anemia, CKD mineral bone disease, erectile dysfunction, decreased immune response against pathogens, pregnancy complications, pericarditis, cancer, metabolic acidosis, hyperuricaemia, endocrine dysfunction and other potential chronic disorders can result from CKD [7]. In severe cases, dialysis and kidney transplantation are the only two treatment options available [8]. Both of these treatment options have a negative impact on patient's health-related quality of life in a variety of ways, including difficulty in finding employment, high rate of infectious complications, increased treatment costs and medicinal side effects [9]. Therefore, compounds derived from natural sources such as plants may provide an alternative treatment system for CKD [10].

In general, Indian medicinal plants have a good reputation among the global scientific community and have contributed numerous bioactive compounds when needed [11]. In this study, compounds from *B. diffusa*, a medicinal plant, cited in Ayurvedha and Siddha literature as a treatment for chronic kidney ailments, were investigated for their potential to treat CKD. Anti-aging, rejuvenating, nourishing, strengthening, and disease-prevention properties of *B. diffusa* phytochemicals are known, implying that they increase health resistance by protecting the body from harmful toxins, such as hepatoprotection, nephroprotection, and immunomodulation [12].

Many experimental studies have shown that *B. diffusa* has diuretic and potentially nephroprotective properties against acetaminophen-induced renal damage [13, 14]. In tribal medicine, a decoction of the roots of the *B. diffusa* plant is used to treat kidney stones. The plant extract contains a variety of secondary metabolites, including flavonoids, glycosides, isoflavonoids, steroids, alkaloids and, phenolic and lignan glycosides [15]. Many rotenoids are also found in the roots of *B. diffusa*. It also has ursolic acids, C-methyl flavone, and punarnavoside, which is a phenolic glycoside. Few reports have indicated that *B. diffusa* provides protection against kidney disease and urolithiasis [16] as well as kidney-regenerating properties [17].

Sodium-glucose Co-transporter-2 (SGLT2), which is mostly found at the brush border of the tubules, is responsible for approximately 90% of the re-absorption of glucose in the proximal tubules [18]. SGLT2 inhibitors, a new class of oral diabetes drugs, are known to lower systolic and diastolic blood pressure, serum uric acid levels, and increase glomerular filtration rate [19]. Because inflammation plays a role in the pathogenesis of CKD, reducing the inflammatory response is a key treatment goal. Furthermore, pleiotropic anti-inflammatory activities of SGLT2 inhibitors appear to be mediated by multiple molecular pathways [20]. The growing importance of bioinformatics and computer-aided drug design approaches is revitalizing today's healthcare systems [21]. Pharmacoinformatics, a set of tools that helps with the groundwork in Drug Discovery and Development, aids in performing *in-silico* analysis of ligand-target interaction, physico-chemical properties and, delegate several preliminary processes such as virtual screening of compounds and targets [22].

Though several studies have suggested that *B. diffusa* can help control CKD, the mechanism of action or the metabolites involved in this process are unknown. As a result, we hypothesized that compounds from *B. diffusa* could effectively mediate the prevention or control of CKD through SGLT2. Molecular modelling tools were used in the current study to identify potential bioactive compounds from *B. diffusa* for the treatment of CKD. SGLT2, a protein linked to CKD was identified as the target. The top binders were identified and their pharmacokinetic and physico-chemical properties were also predicted and assessed using web-based tools. The present work describes an effort to discover a therapy for CKD by utilizing common folklore plant with medicinal value that have been demonstrated through various empirical studies investigating their curative/prophylactic properties.

2. RESULTS

2.1. Ligand-binding site prediction and receptor grid formation

Nineteen potential binding sites (AS1-AS19) were predicted by analysis of the protein, SGLT2. In Table 1, the ligand binding pockets were listed together with their amino acid residues, rank, score,

likelihood, and X, Y, and Z dimension values. The prediction of binding pockets would help in setting up a grid for ligand binding in the target protein during molecular docking. Based on the prediction analysis, AS1 with the grid box dimensions of X = 37.97, Y = 52.58, and Z = 49.47 in angstrom (Å) has been selected based on its high score and probability value.

Table 1. PrankWeb tool used to prediction of binding pockets and correspondence binding sites of SGLT2 enzyme. The first pocket is coloured in blue with pocket score of 56.67, 55 amino acids and a probability score of 0.956.

Name	Rank	Score	Probability	X axis	Y axis	Z axis	Amino acid residues
pocket1	1	56.67	0.956	37.9778	52.5886	49.4717	A_153 A_154 A_157 A_158 A_255 A_256 A_257 A_259 A_273 A_274 A_283 A_286 A_287 A_290 A_291 A_296 A_297 A_336 A_343 A_344 A_345 A_346 A_359 A_360 A_361 A_362 A_363 A_396 A_397 A_449 A_450 A_451 A_453 A_454 A_457 A_460 A_508 A_509 A_510 A_511 A_526 A_74 A_75 A_79 A_80 A_83 A_84 A_86 A_87 A_89 A_90 A_91 A_95 A_98 A_99
pocket2	2	10.01	0.367	34.3364	53.4799	63.0763	A_160 A_164 A_167 A_168 A_174 A_355 A_356 A_357 A_359 A_360 A_361 A_362 A_363 A_364 A_445 A_447 A_448 A_449
pocket3	3	9.32	0.332	50.803	20.2521	39.684	A_127 A_130 A_136 A_139 A_407 A_411 A_412 A_414 A_415 A_417 A_418 A_419 A_422 A_52 A_574 A_575 A_578 A_579 A_580 A_581 A_593
pocket4	4	7.58	0.24	46.6564	46.3277	32.0799	A_108 A_112 A_113 A_284 A_285 A_288 A_292 A_468 A_472 A_476 A_534
pocket5	5	6.79	0.2	48.9153	59.4518	52.6411	A_451 A_454 A_455 A_458 A_499 A_500 A_503 A_504 A_507 A_508 A_509 A_515 A_517 A_522 A_524 A_525 A_526
pocket6	6	6.43	0.183	46.8592	48.8105	58.0613	A_152 A_156 A_440 A_443 A_444 A_447 A_451 A_452 A_455 A_503 A_504 A_507 A_508
pocket7	7	5.94	0.16	25.6102	33.9638	26.9373	A_308 A_309 A_312 A_315 A_316 A_64 A_649 A_652 A_653 A_656
pocket8	8	5.09	0.125	23.8217	38.0443	61.41	A_166 A_170 A_172 A_177 A_181 A_184 A_22 A_25 A_26 A_29 A_33 A_383 A_384 A_386 A_387

pocket9	9	3.98	0.082	28.0489	24.0455	51.6769	A_187 A_188 A_191 A_36 A_37 A_40 A_41 A_44 A_622
pocket10	10	3.86	0.078	44.2763	20.6159	33.3861	A_120 A_121 A_122 A_123 A_131 A_52 A_53 A_57 A_580 A_581 A_582 A_583 A_586 A_636 A_637 A_638 A_640 A_641
pocket11	11	3.27	0.056	17.3408	36.6524	51.932	A_206 A_207 A_211 A_28 A_31 A_32 A_35 A_381 A_384
pocket12	12	3.24	0.055	53.8183	46.0533	52.7819	A_145 A_148 A_152 A_440 A_455 A_463 A_493 A_497 A_500 A_504
pocket13	13	2.7	0.038	51.1028	32.7607	53.7179	A_144 A_147 A_148 A_151 A_405 A_409 A_429 A_432 A_433 A_436
pocket14	14	1.82	0.015	23.2787	37.4471	38.3417	A_202 A_205 A_206 A_209 A_316 A_320 A_65 A_69
pocket15	15	1.67	0.012	43.0796	-3.7595	53.6699	A_598 A_599 A_603 A_605 A_607 A_610
pocket16	16	1.58	0.01	38.0731	55.075	32.2113	A_101 A_104 A_280 A_284 A_668
pocket17	17	1.54	0.009	27.2173	28.5911	55.578	A_184 A_187 A_188 A_191 A_33 A_36 A_37 A_391
pocket18	18	1.14	0.004	25.3503	45.7552	44.9593	A_208 A_323 A_327 A_328 A_72
pocket19	19	0.8	0.001	23.9519	63.6758	37.8804	A_226 A_230 A_263 A_670 A_671

2.2. Protein preparation

The selected models were evaluated using the Ramachandran plot (Supplementary Figure 1) under the structure assessment page in Swiss Mode itself. An energetically preferred location for backbone dihedral angles against amino acid residues in protein structure can be seen using a Ramachandran map. It determines the contours of favoured regions, based on the number of observed Φ / Ψ pairs. The modeled structure received a MolProbity score of 1.45 and clash score of 0.89 with both having a good cutoff value ≥ 66 percentile. The Ramachandran favored is 94.46% with cutoff value of $\geq 98\%$ considered good. Then the 3D PDB file was retrieved. Figure 1 shows the 3D structure of SGLT2 modelled using Swiss Model server.

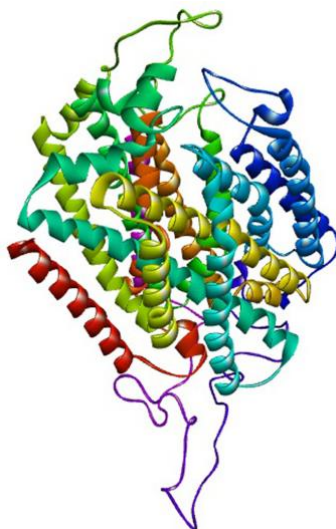
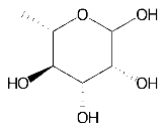


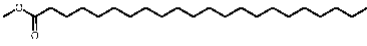
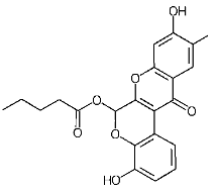
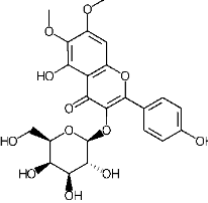
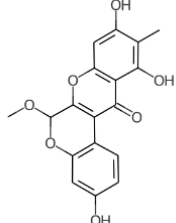


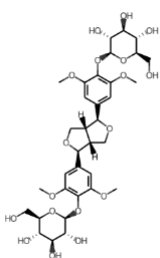
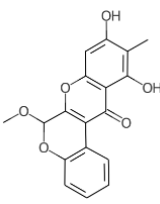
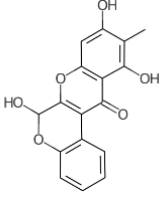
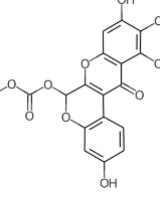
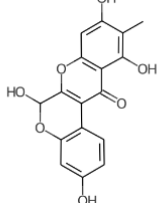
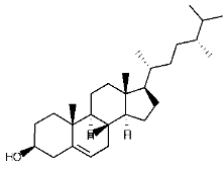
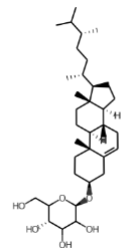
Figure 1. The 3D structure of the modeled target protein Sodium/ glucose co-transporter 2 using Swiss Model.

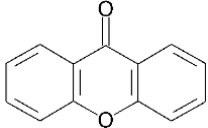
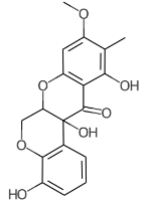
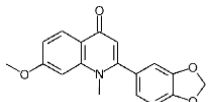
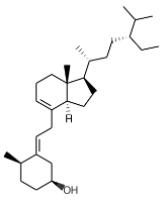
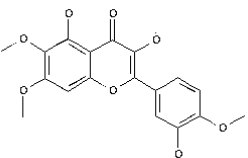
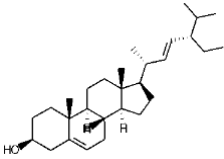
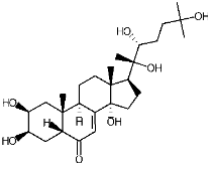
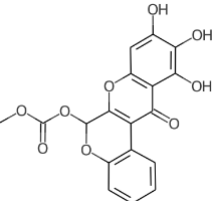
2.3. Molecular docking

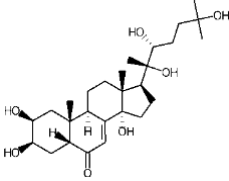
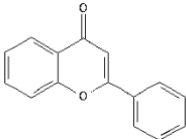
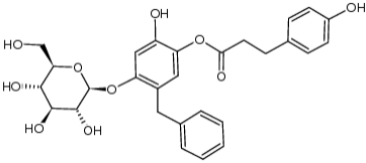
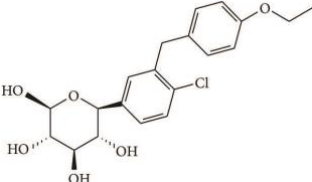
The AutoDock Vina wizard in the PyRx programme was used to perform molecular docking of the 25 phytochemicals of *B. diffusa* at the selected binding site, AS1, of the chosen target protein (SGLT2). According to molecular docking, the binding energies required for the binding of phytochemicals to the target protein ranged from -6.1 to -10.6 kcal \times mol⁻¹. Punarnavoside (-10.2 kcal \times mol⁻¹) and flavone (-9.3 kcal \times mol⁻¹), which have binding affinity closer to the standard drug, dapaglifozin (-10.6 kcal \times mol⁻¹), were selected as the high binding compounds out of the 25 phytochemicals evaluated for binding to SGLT2. The binding affinities of all the ligands against SGLT2 along with the binding affinity of the standard drug, dapaglifozin are presented in Table 2.

Table 2. Bioactive molecules from *Boerhavia diffusa* and standard drug with their binding affinity against sodium/glucose co-transporter 2 (SGLT2) enzyme.

S. No	Bioactive molecule	Structure	Binding Affinity (kcal \times mol ⁻¹)
1	L-Rhamnose		-6.1
2	Hentriacontane		-6.4
3	1-Triacontanol		-6.5
4	Methyl behenate		-6.6
5	Diffusarotenoid		-7.4
6	Betuletrin		-7.7
7	Boeravinone D		-7.7

8	Liriodendrin		-7.9
9	Boeravinone A		-8.1
10	Boeravinone B		-8.2
11	Repenol		-8.2
12	Boeravinone E		-8.2
13	Campesterol		-8.2
14	Campesterol glucoside		-8.2

15	Xanthone		-8.5
16	Boeravinone C		-8.6
17	Lunamarine		-8.6
18	Boerhavisterol		-8.6
19	Eupalitin		-8.7
20	Stigmasterol		-8.8
21	Ecdysterone		-8.8
22	Repenone		-8.9

23	20-Hydroxyecdysone		-8.9
24	Flavone		-9.3
25	Punarnavoside		-10.2
26	Dapaglifozin		-10.6

Standard drug

2.4. Interpretations of protein–ligands interaction

The amino acids of the target protein interacting with the lead phytochemicals have been viewed through BIOVIA Discovery studio visualizer tool. The top-scoring phytochemical, punarnavoside (docking score: $-10.2 \text{ kcal} \times \text{mol}^{-1}$), formed strong contacts with the target, SGLT2, as shown in Figure 2 and Table 3 by nine hydrophobic interactions [THR87A (3.97Å), VAL95A (2.95Å), PHE98A (3.49Å), PHE98A (3.73Å), LYS154A (3.44Å), LYS154A (3.65Å), VAL157A (3.53Å), LEU274A (3.94Å) and GLN457A (3.56Å)], one salt bridges (HIS80A (5.34Å)), and seven hydrogen bonding interactions (ASN75A (2.40Å), PHE98A (2.04Å), TRP291A (2.47Å), LYS321A (2.81Å), ASP454A (2.35Å), GLN457A (2.02Å) and TYR526A (3.13Å)).

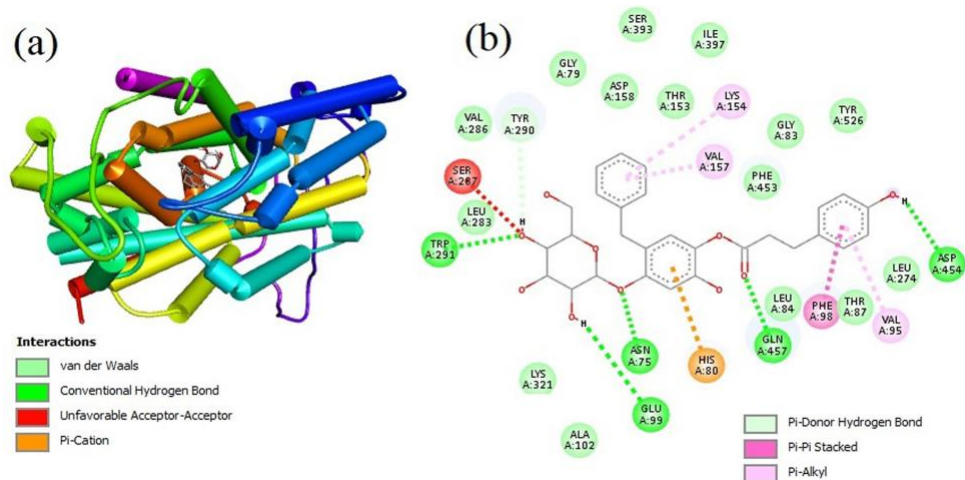


Table 3. Details of bonding interactions between Sodium-Glucose Co-transporter 2 enzymes with selected bioactive molecules Punarnavoside, Flavone and standard drug Dapaglifozin.

Bioactive molecule	Residues	Amino Acid	Distance (Å)	Bond Category	
Punarnavoside	87A	THR	3.97	Hydrophobic Interactions	
	95A	VAL	2.95		
	98A	PHE	3.49		
	98A	PHE	3.73		
	154A	LYS	3.44		
	154A	LYS	3.65		
	157A	VAL	3.53		
	274A	LEU	3.94		
	457A	GL004E	3.56		
	75A	ASN	2.4		
	98A	PHE	2.04		
	291A	TRP	2.47		
	321A	LYS	2.89		Hydrogen Bonds
	454A	ASP	2.35		
	457A	GLN	2.02		
526A	TYR	3.13	Salt Bridges		
80A	HIS	5.34			
84A	LEU	3.99			
95A	VAL	3.8			
98A	PHE	3.58			
98A	PHE	3.77			
98A	PHE	3.94		Hydrophobic Interactions	
290A	TYR	3.82			
290A	TYR	3.57			
453A	PHE	3.98		Hydrophobic Interactions	
457A	GLN	3.95			
84A	LEU	3.51			
87A	THR	3.73			
95A	VAL	3.59			
98A	PHE	3.84			
98A	PHE	3.63			
98A	PHE	3.7			
274A	LEU	3.75			
453A	PHE	3.8			
457A	GLN	3.66			

87A	THR	3	
99A	GLU	3.49	
286A	VAL	3.35	
287A	SER	3.17	Hydrogen Bonds
457A	GLN	2.39	
460A	SER	2.06	
460A	SER	2.32	
80A	HIS	4.49	π -cation
79A	GLY	3.04	Halogen Bonds

2.5. Pharmacokinetics and physico-chemical properties of bioactive compounds

The SwissADME online tool was used to predict the pharmacokinetics and physico-chemical characteristics of the top scoring bioactive compounds, punarnavoside and flavone from *B. diffusa* and the standard drug, dapaglifozin and, the results are shown in Table 4. As presented in Table 4, the selected top binder, punarnavoside (molecular weight: 526.53 g \times mol⁻¹), was found to contain two violations for Lipinski's rule of five and, flavone (molecular weight: 222.24 g \times mol⁻¹) was found to have zero violations, and the standard drug dapaglifozin (molecular weight: 408.87 g \times mol⁻¹) was observed with zero violations of Lipinski's rule of five. The observed numbers of violations in punarnavoside were due to higher molecular weight (>500 g \times mol⁻¹) and more than 5 hydrogen bond donors (NH or OH > 5). The polar surface area of punarnavoside and flavone were 166.14 Å² & 30.21 Å² respectively, and for dapaglifozin it was 99.38 Å². The gastrointestinal absorption (GI) property was low for punarnavoside whereas the flavone and standard drug, dapaglifozin exhibited high gastrointestinal (GI) absorption. Hence, to use punarnavoside as a drug, few formulation strategies need to be adapted which could enhance its GI absorption or could be formulated into sustained - release and delayed release dosage forms. Based on the observed results, punarnavoside, flavone and dapaglifozin demonstrated a positive bioavailability score of +0.17, +0.55 and +0.55 respectively. Based on this information, it can be concluded that punarnavoside and flavone have a better chance as a possible drug-like candidates for the treatment of CKD. The synthetic accessibility score for punarnavoside, flavone and dapaglifozin were found to be 5.53, 2.88 and 4.52, respectively, which represents the possibility for synthesis, as the ability to synthesize biomolecules in the laboratory is based on scoring range from 1 (very easy) to 10 (very difficult to synthesize).

Table 4. Pharmacokinetics and physicochemical parameters of selected top binding scored bioactive molecule punarnavoside, flavone and standard drug dapaglifozin

Parameters	Punarnavoside	Flavone	Dapaglifozin
Formula	C ₂₈ H ₃₀ O ₁₀	C ₁₅ H ₁₀ O ₂	C ₂₁ H ₂₅ ClO ₆
MW (g mol ⁻¹)	526.53	222.24	408.87
Num. heavy atoms	38	17	28
Num. aromatic heavy atoms	18	16	12
Fraction Csp ³	0.32	0	0.43
Num. rotatable bonds	10	1	6

Num. H-bond acceptors	10	2	6
Num. H-bond donors	6	0	4
Molar Refractivity	134.88	67.92	104.82
TPSA (Å ²)	166.14	30.21	99.38
Solubility	Moderately soluble	Moderately soluble	Moderately soluble
GI absorption	Low	High	High
BBB permeation	No	Yes	No
Violation of Lipinski's rule of five	2	0	0
Violation of Veber rule	1	0	1
Bioavailability Score	0.17	0.55	0.55
Synthetic accessibility	5.53	2.88	4.52

Figure 5 presents the visual representation of the drug-likeness of the top binding compounds. An ideal range for bioactive compounds is the pink region inside the hexagon of the illustration. For the drug-like molecule, the optimal range was as follows: saturation (SATU): fraction of carbons in the sp³ hybridization not less than 0.25; insolubility (INSOLU): log S not higher than 6; molecular weight (SIZE): between 150 and 500 g × mol⁻¹; hydrophobicity (LIPO): XLOGP3 between -0.7 and +5.0, rotatable bonds (FLEXI): no more than 9 rotatable bonds and polar surface area (POLAR): TPSA between 20 and 130 Å².

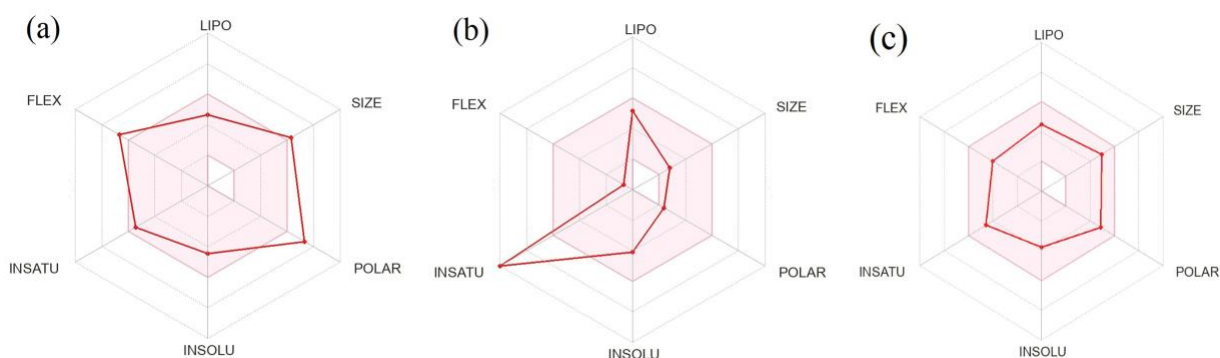


Figure 5. Bioavailability radar plot for oral bioavailability of top binding scored bioactive molecules. Punarnavoside (a), flavone (b) and standard drug Dapaglifozin (c). The pink area exhibits the optimal range for each properties (Lipophilicity as XLOGP3 between -0.7 and +5.0; Size as molecular weight between 150 and 500 g mol⁻¹; Polarity as TPSA (topological polar surface area) between 20 and 130 Å²; Insolubility in water by log S scale not higher than 6; Insaturation as per fraction of carbons in the sp³ hybridization not less than 0.25 and Flexibility as per rotatable bonds no more than 9).

The boiled-egg model was also used to examine the pharmacokinetic characteristics of punarnavoside, flavone and the commonly used drug, dapaglifozin and the results are presented in Figure 6. As depicted in Figure 6, the bioactive molecule, punarnavoside, was found to be present outside albumin

(white region), which revealed a lower absorption in the gastrointestinal tract, whereas flavone was observed in the yellow region (yolk) of the boiled-egg one, and they might be able to cross BBB. Based on these findings, it can be interpreted that the bioactive molecule, punarnavoside, needs formulation strategies to improve its absorption and solubility parameters before using this as a potential drug candidate.

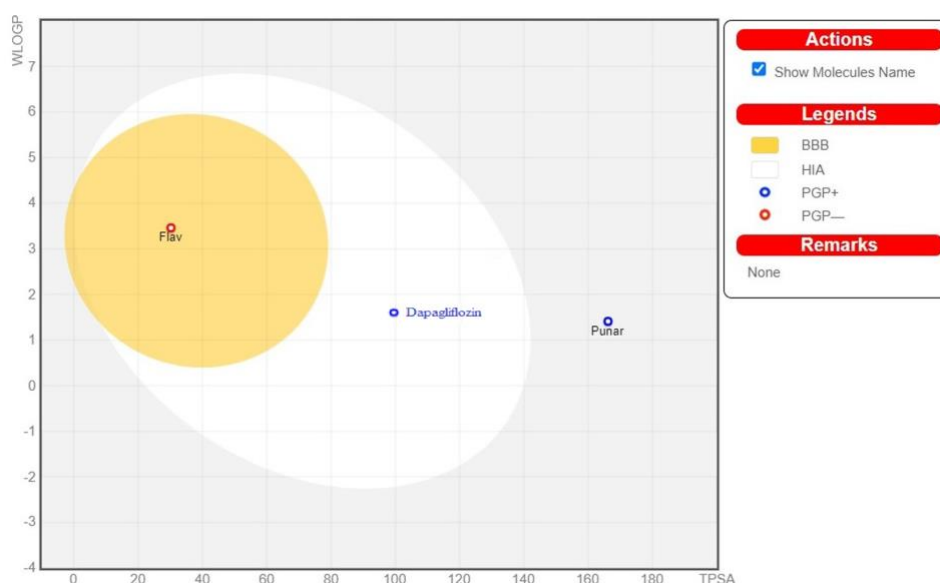


Figure 6. The EGG-BOILED model for the bioactive molecule Punarnavoside, Flavone and the standard drug Dapagliflozin. The EGG-BOILED represents for intuitive evaluation of passive gastrointestinal absorption (HIA) white part and blood brain penetration (BBB) yellow part as well as substrates (PGP+) and non-substrates (PGP-) of the permeability glycoprotein (PGP) are represented by blue and red color circles, respectively, of the selected top binding scored bioactive molecule Punarnavoside and standard drug Dapagliflozin in the WLOGP-versus-TPSA graph. The grey region is the physicochemical space of compounds predicted to exhibit high intestinal absorption.

2.6. Toxicity profile

An *in-silico* toxicity test utilizing the pkCSM web server has been carried out to determine the toxic effects of the selected bioactive compounds, punarnavoside and flavone, along with the standard drug, dapagliflozin. Tetrahymena pyriformis (TP) toxicity, carcinogenicity, hepatotoxicity, PGI, oral rat acute toxicity (LD_{50}), and oral rat chronic toxicity (LOAEL) have all been performed using the server and the results are presented in Table 5. From Table 5, we could identify that the selected top binding molecule, punarnavoside, have not exhibited AMES toxicity which implies that the compound is non-mutagenic, while flavone showed AMES toxicity. The inward rectifying voltage gated potassium channel in the heart (IKr), which is important in cardiac repolarization, is encoded by the human ether-a-go-go related gene (hERG). Hence, it is important for drug candidates not to be a hERG inhibitor and punarnavoside and flavone have no hERG inhibition. Punarnavoside and flavone were predicted not to induce hepatotoxicity. Punarnavoside and flavone were also reported “no” for skin sensitization which is another important parameter for a drug. The maximum recommended tolerated dose of punarnavoside and flavone were found to be 0.225 and 0.033 log mg/kg/day, respectively. Similarly, the lethal dosage (LD_{50}) of punarnavoside and flavone were identified as 2.689 & 1.997 mol \times kg⁻¹, respectively, and Oral Rat Chronic Toxicity (LOAEL) was 3.59 & 1.015 log mg \times kg⁻¹ b.w/day, respectively. The *T. pyriformis* toxicity of punarnavoside and flavone were predicted to be 0.285 & 0.774 log μ g \times L⁻¹ and the Minnow toxicity as -0.263 & 0.763 log mM, respectively, which implies that both the compounds are safe and non-toxic and could effectively be used as a drug compounds.

Table 5. List of the drug-induced hERG inhibition, AMES toxicity, carcinogens, Tetrahymena pyriformis (TP) toxicity, rat acute toxicity (LD₅₀ in mol kg⁻¹), and skin sensitisation along with Minnow toxicity of punarnavoside, Flavone and standard drug dapaglifozin.

Parameters	Punarnavoside	Flavone	Dapaglifozin
AMES toxicity	No	Yes	No
Max. tolerated dose (human) (log mg/kg/day)	0.225	0.033	0.507
hERG inhibition	No	No	No
Oral Rat Acute Toxicity LD ₅₀ (mol kg ⁻¹)	2.689	1.997	2.475
Hepatotoxicity	No	No	No
Oral Rat Chronic Toxicity (LOAEL) (log mg/kg b.w/day)	3.59	1.015	3.63
Skin Sensitisation	No	No	No
T. pyriformis toxicity (log ug L ⁻¹)	0.285	0.774	0.289
Minnow toxicity (log mM)	-0.263	0.763	1.079

2.7. Molecular dynamics simulation

MD simulations were carried out for punarnavoside-SGLT2 complex, flavone-SGLT2 complex and dapaglifozin-SGLT2 complex to evaluate the stability of these complexes.

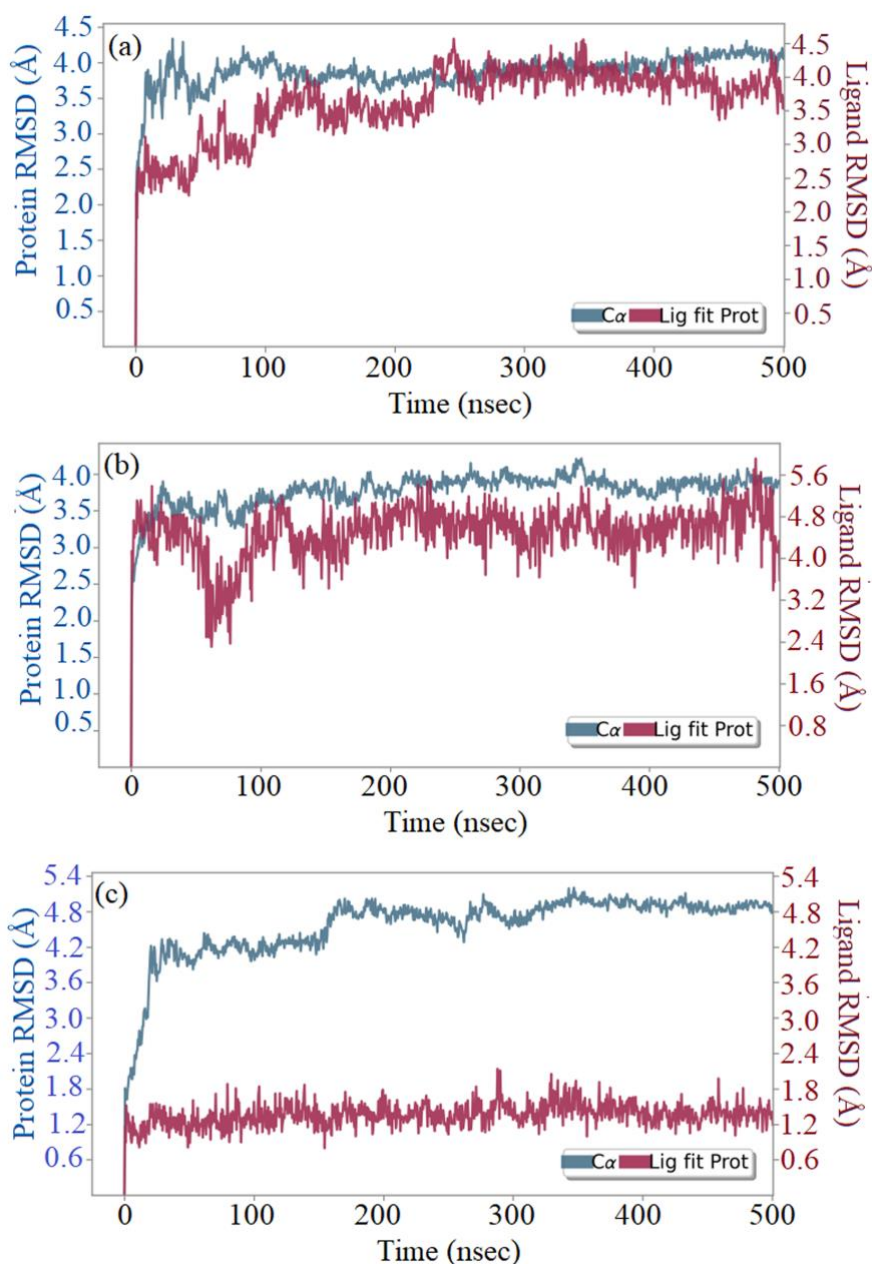


Figure 7. RMSD study plot for 100ns MD Simulation of SGLT2–Punarnavoside docked complex (a), SGLT2–Flavone docked complex (b), and SGLT2–Dapaglifozin docked complex (c).

The trajectory events of punarnavoside-SGLT2 complex revealed that the RMSD of the protein fluctuated up to 4.5 Å but the ligand complex fluctuated to 3 Å and retained its stability throughout the simulation period (Figure 7(a)). The protein-ligand complex revealed that the amino acid residues, ASN75 (58%), HIS80 (99%), PHE98 (35%), GLU99 (72%), SER287 (70%), TYR290 (28%), LYS321 (95%), TYR526 (14%), ASP454 (63%) and GLN457 (96%) contribute for maximum interaction with punarnavoside and, also for its stability (Figure 8 (a, b)). Since the GLN457, SER287, GLU99, and HIS 80 were having higher interactions with punarnavoside, and these amino acids are present in the binding sites of SGLT2, thus punarnavoside may significantly contribute to the stability and the potency of SGLT2 inhibition.

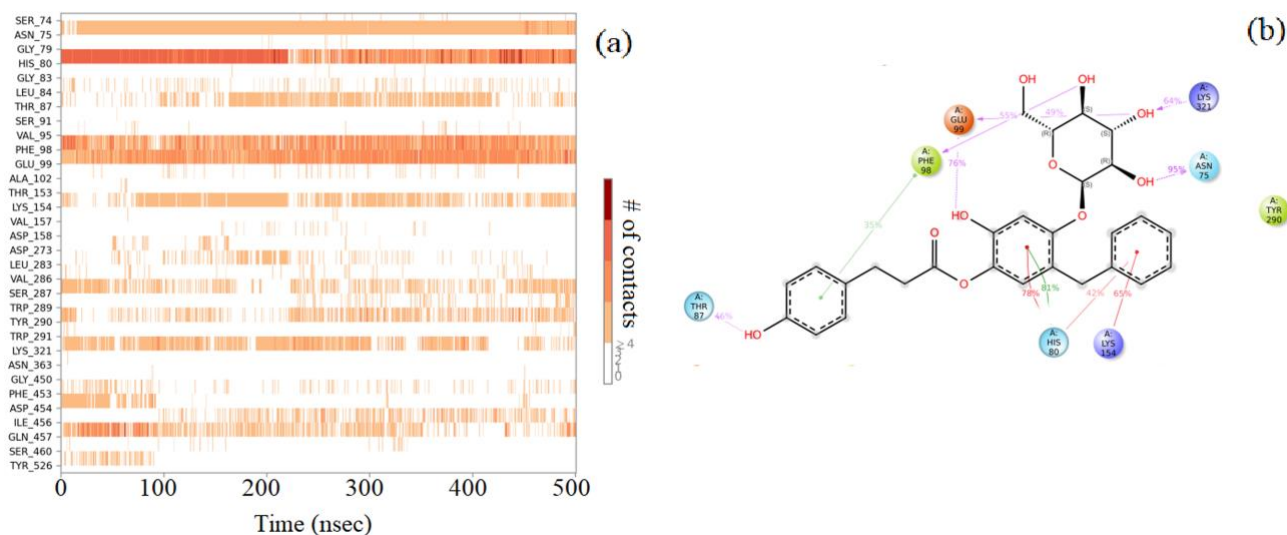


Figure 8. SGLT2-Punarnavoside contacts timeline representation (a); and Punarnavoside contacts with respective to the amino acids in the target SGLT2 (b).

The flavone-SGLT2 complex MD trajectory events revealed that the protein RMSD fluctuated between 2.4 Å and 3.6 Å (Figure 7(b)). Ligand RMSD fluctuations were between 3.2 and 4 Å, indicating that it was stable. The flavone-SGLT2 protein contacts showed that amino acid residues TYR290 (55%), and LEU84 (44%) contribute maximum to the interaction with flavone (Figures 9 (a, b)). TYR290 and LEU84 were having higher interactions with flavone, and these amino acids are present in the binding sites of SGLT2, thus flavone may contribute to the stability and the effective of SGLT2 inhibition.

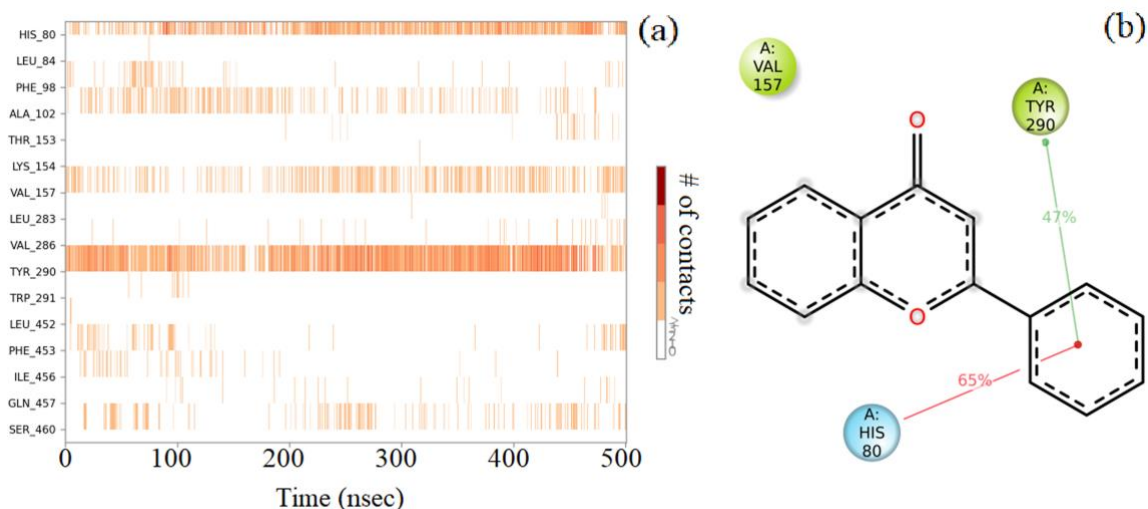


Figure 9. SGLT2-Flavone contacts timeline representation (a); and Flavone contacts with respective to the amino acids in the target SGLT2 (b).

The trajectory events of dapaglifozin-SGLT2 complex revealed that the protein RMSD fluctuated up to 4.2 Å but the ligand complex fluctuated to 1.8 Å and retained its stability throughout the simulation period (Figure 7 (c)). The analysis of protein-ligand complex revealed that amino acid residues LYS321 (99%), SER287 (83%), GLU99 (66%), PHE98 (60%), and GLN457 (64%) contribute to higher interaction with dapaglifozin leading to the stability of the complex (Figure 10 (a, b)). The amino acids, SER287, GLU99, PHE98 and GLN457 were having higher interactions with dapaglifozin, and these are present in the binding sites of SGLT2, thus dapaglifozin significantly contribute to the stability and the potency of SGLT2 inhibition.

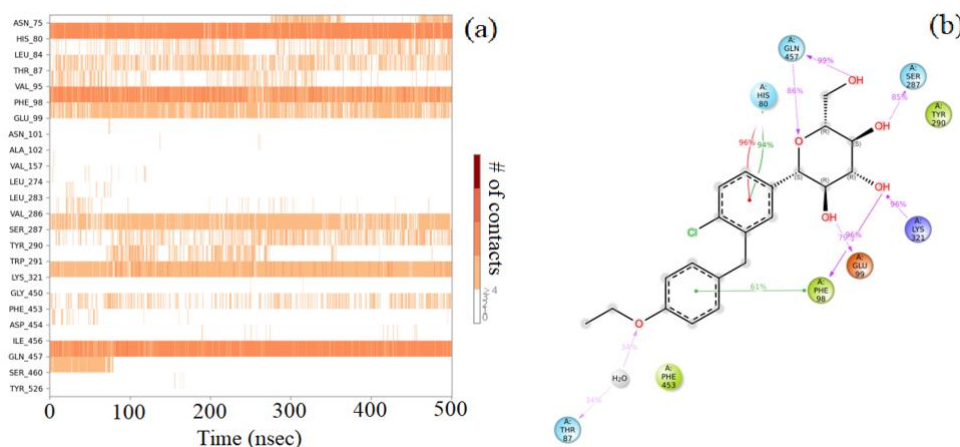


Figure 10. SGLT2-Dapagliflozin contacts timeline representation (a); and Dapagliflozin contacts with respective to the amino acids in the target SGLT2 (b).

No major fluctuations were observed in RMSF analysis of all complexes with the key amino acids (Figure 11). Aromatic pi-pi stacking and hydroxy substitution play a major role in interacting with the key amino acids.

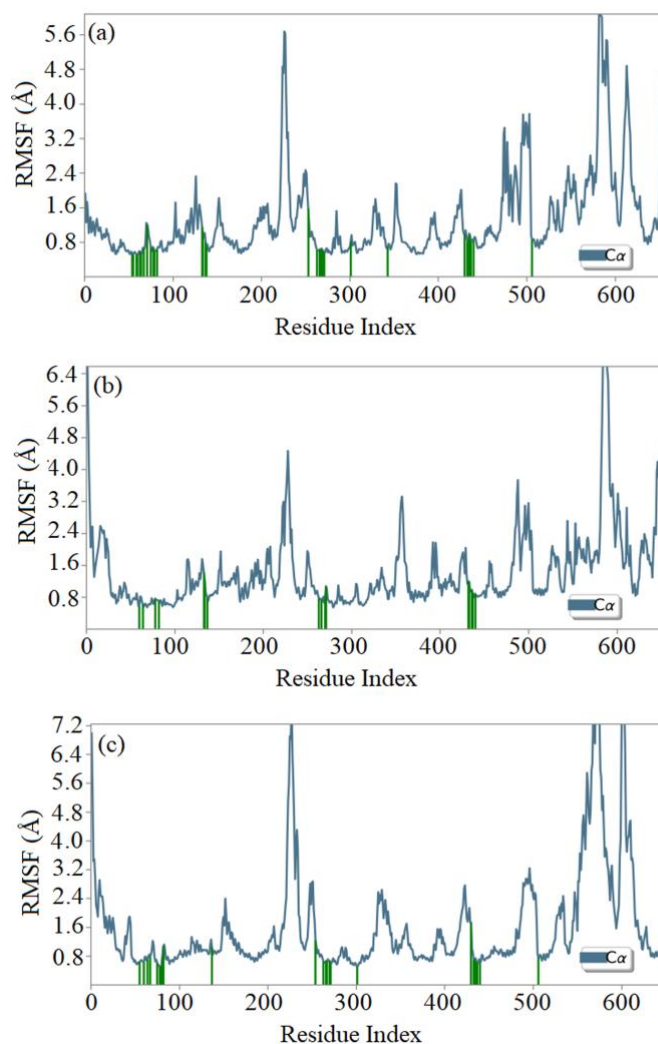


Figure 11. RMSF of the Punarnavoside for characterizing changes in the ligand atom positions (a), RMSF of the Flavone for characterizing changes in the ligand atom positions (b), RMSF of the Dapagliflozin for characterizing changes in the ligand atom positions (c).

Timeline representations (H-bonds, hydrophobic, ionic, water bridges) of all the amino acid residues were also observed in Figure 12. The darker lines indicated that the continuous interactions with the target. All these interactions made the protein-ligand complex stable throughout the entire duration of MD simulation study. The MD simulation analysis clearly indicates that punarnavoside could be a better lead candidate against CKD and could further be evaluated using in vitro and in vivo assays.

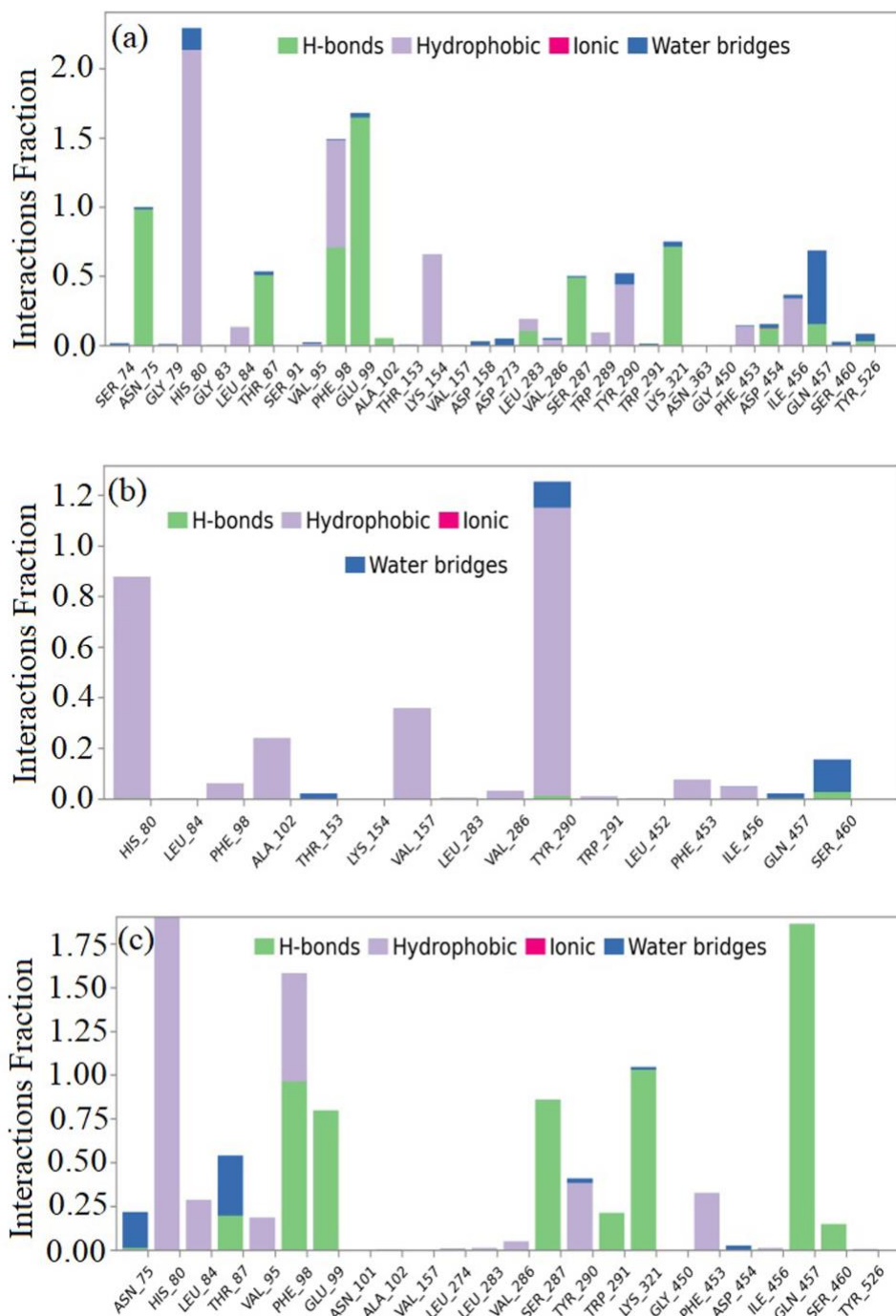


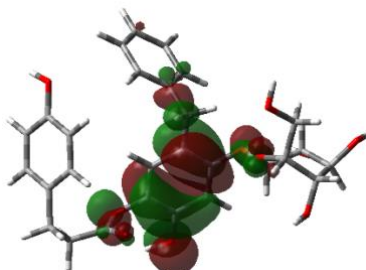
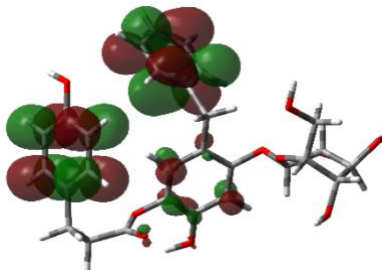
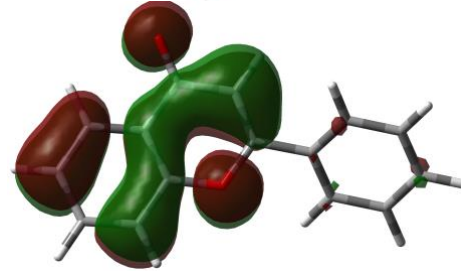
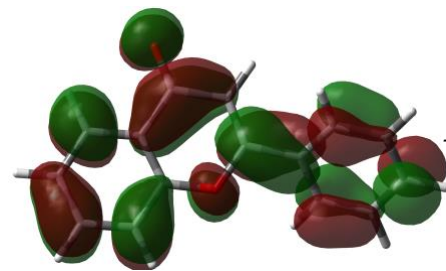
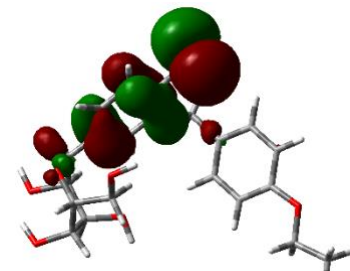
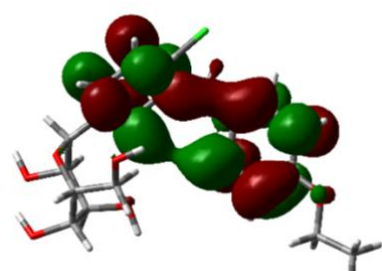
Figure 12. Amino acid and water mediated interactions with the ligands, Punarnavoside (a), flavone (b), and standard drug Dapaglifozin (c).

2.8. Density functionality theory analysis

Most importantly, the highest occupied molecular orbital (HOMO) and lowest unoccupied molecular orbital (LUMO) are vital, their energies and HOMO–LUMO energy gap are calculated by B3LYP

level with 6-311G (d, p) basis set and the HOMO–LUMO pictures of the top scored compounds, punarnavoside, flavone and the reference drug, dapagliflozin are presented in Table 6. The energy values of the lowest unoccupied molecular orbital (E_{LUMO}) and the highest occupied molecular orbital (E_{HOMO}) and their energy gap (ΔE) reflect the chemical reactivity of the molecule. Recently the energy gap between HOMO and LUMO has been used to prove the bioactivity from intramolecular charge transfer (ICT). The top scored compounds, punarnavoside and flavone, were found to have more energy band gap, and this could be the reason for its increased bioactivity.

Table 6. E_{HOMO} and E_{LUMO} and ΔE values of selected top binding scored compounds, Punarnavoside, Flavone and standard drug Dapagliflozin.

Compound Name	HOMO	E_{HOMO} (ev)	LUMO	E_{LUMO} (ev)	Energy gap (ΔE)
Punarnavoside		-8.75		-5.17	3.58
Flavone		-9.38		-5.98	3.40
Dapagliflozin		-8.2918		-5.1568	3.1350

2.9. Metabolite prediction and molecular docking

The tool, SmartCYP, assists in comprehending various sites in a compound which are liable for metabolism due to cytochrome isoforms (CYP3A4, CYP2D6, and CYP2C9). As analysed by SmartCYP, energy of the compound punarnavoside is less than $999 \text{ kJ} \times \text{mol}^{-1}$ and similarity lies between 0 and 1. A total of 15 sites of cytochrome P450 metabolism were identified by the SmartCYP and out of which the top three sites of metabolism were found at C5, C2 and C14 respectively as depicted in Figure 13.

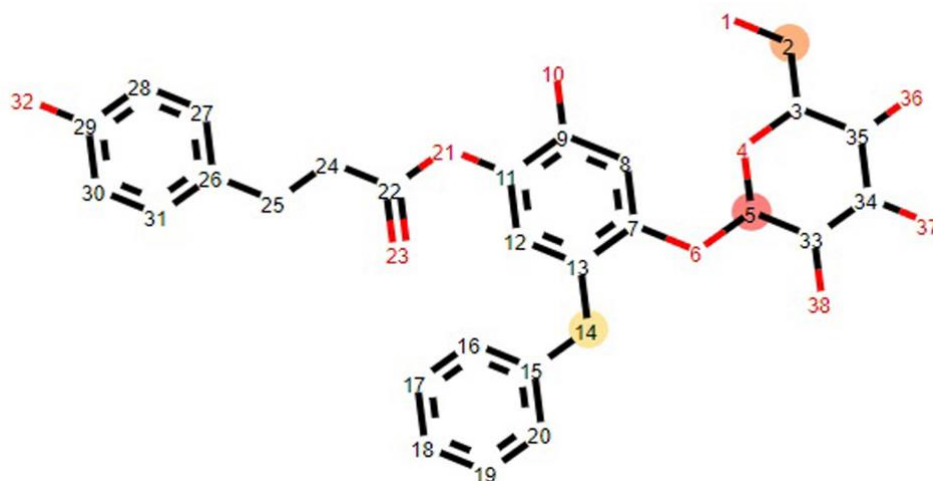


Figure 13. Metabolic site prediction and Atom numbering of punarnavoside by SMARTCyp web server.

The Chemsketch tool was then used to draw the three metabolites of punarnavoside (Figure 14) based on the top three sites of metabolism inferred from SmartCYP. The AutoDock Vina wizard in the PyRx programme was used to perform molecular docking between the three metabolites of punarnavoside against the predicted binding site, AS1 of the chosen target protein (SGLT2). According to the results of molecular docking, binding affinities of the metabolites to the target protein ranged from -9.4 to -10.3 kcal \times mol⁻¹ in AS1 (Supplementary Table 1). Among the metabolites, punarnavoside 1 (PS1) showed better binding affinity of -10.3 kcal \times mol⁻¹, which is close to the lead molecule (Punarnavoside: -10.2 kcal \times mol⁻¹).

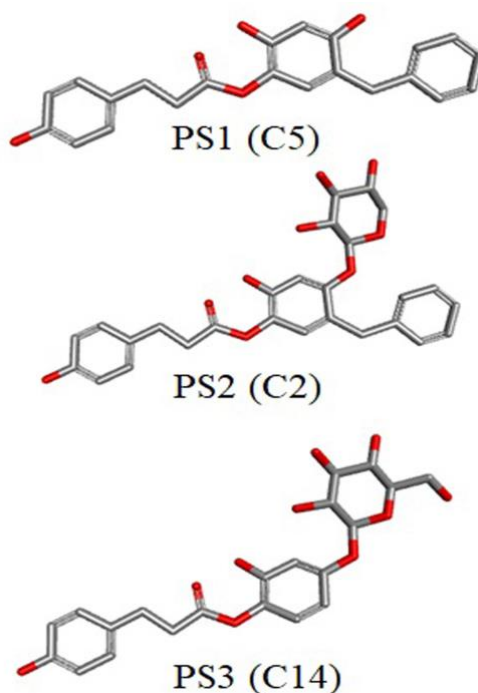


Figure 14. Predicted metabolites of punarnavoside by cytochrome P450 metabolism pathway

3. DISCUSSION

The current study sought to identify plant-based molecules that could be helpful in the treatment/prevention of chronic kidney disease (CKD). Diabetes, free radical formation, hypertension, kidney infections and drug induced toxicity are the most common causes of CKD [23]. Many plant-derived compounds from medicinal plants or the plant extracts have been used to treat various ailments. Similarly, effective treatment/prevention of CKD using various bioactive plant components has been reported. For instance, curcumin (*Curcuma longa*) in combination with thymoquinone (*Nigella sativa*), daphnetin (*Daphne odora*), dioscin (*Dioscorea zingiberensis*) and, embelin (*Embelia ribes*) are known to prevent CKD. *B. diffusa*

contains numerous bioactive components that are commonly used as antioxidants, diabetes preventives, and nephroprotectives [24]. Because of the prediction capabilities of *in-silico* molecular docking tools, the development of effective drugs for disease prevention could be faster [25]. Using a collection of *in-silico* molecular docking methods, it is possible to screen these medicinally important bioactive molecules that are useful for preventing renal failure. Higher predictive scores of binding energy against the target protein, molecular dynamics simulation studies, pharmacokinetic, physiochemical, and pharmacodynamic features would significantly aid in the search for potential nephroprotective drugs [26, 27]. These findings could then be validated using *in vitro* and *in vivo*.

Based on the literature, sodium/glucose co-transporter 2 (SGLT2) was chosen as an ideal therapeutic target for CKD in the current study. Various studies have shown that inhibition of SGLT2 improves glomerular hemodynamic function while also improving various regional and systemic pathways implicated in the etiology of CKD and cardiovascular disease (CVD) [28].

The objective of this study was to identify bioactive compounds from *B. diffusa* that could inhibit the activities of the chosen target, SGLT2. Using the IMPPAT database, twenty-five phytochemicals from *B. diffusa* were chosen. Bioinformatics tools that help researchers understand how phytochemicals bind, interact, and inhibit/stimulate a specific protein may aid in the discovery of therapeutic options for certain disease conditions. A protein's ligand binding site is defined by the presence of specific amino acid residues that form intermediary bonds with the ligand [29]. The docking scores of the chosen phytochemicals against the SGLT2 protein ranged between -8.2 to -10.6 kcal \times mol⁻¹. Punarnavoside (-10.2 kcal \times mol⁻¹) and flavone (-9.3 kcal \times mol⁻¹) have been chosen for further investigation because of their potential binding ability, strong hydrogen and hydrophobic bonding interactions with amino acid residues present in the active site of SGLT2. One of the most important interactions between the biologically active compounds and protein is the hydrogen bond. Hydrogen bonds support the three-dimensional structure of proteins and nucleic acids, aid in biological recognition, and are intimately linked to the rapid creation and dissolution of molecules required for biological activities.

Pharmacokinetic and physicochemical properties are evaluated for any new drug being developed because they are directly related to the bioavailability and effectiveness of the phytochemical [30]. To elicit effective biological responses, physiologically active phytochemicals must be present in sufficient quantities and for an extended period at the site of illness or target site. To pass the required clinical trials and be considered a prospective therapeutic candidate, the pharmacokinetic and physicochemical characteristics of the bioactive compounds must be improved during the drug development process [31]. Furthermore, it appears that the Lipinski Rule of Five technique can be used to predict the drug-like qualities of phytochemicals [32].

Molecular weight and polar surface topological area (TPSA) have been identified as pharmacokinetic factors that control the permeability of bioactive chemicals through biological barriers [33]. The permeability of the bioactive molecule may be reduced due its higher molecular weight and lower TPSA [34]. Lipophilicity and solubility influence the body's ability to absorb phytochemicals [35]. Punarnavoside, the selected bioactive compound, has lower gastrointestinal absorption due its higher molecular weight. The number of hydrogen bond acceptors/donors in the phytochemical influences its permeability [36].

Phytochemicals with 12 or fewer hydrogen bond donors are recommended for effective permeability of biological barrier. During this investigation, the chosen lead molecule, punarnavoside, was found to have 10 hydrogen bond acceptors and 6 hydrogen donors. This indicates that this molecule has a low permeability through biological barriers. Furthermore, phytochemicals with high oral bioavailability are thought to have 10 rotatable bonds. The boiled-egg test was used to determine permeability across the blood-brain barrier and human intestine absorption of the selected bioactive compound. The chosen phytochemical was also tested for its pharmacokinetics and physicochemical characteristics, and the results were used to guide subsequent assessment tests.

To investigate the potentially harmful effects of a phytochemical on the host organism, their toxicity must be determined. Because toxicology and severe adverse reactions are the most common reasons for medication failure during late-stage drug development, it is an important stage in the design and development of candidate drugs. The hazardous profile of phytochemicals must be investigated using *in vitro* and *in vivo* animal models; however, these investigations are time-consuming, expensive, and difficult due to ethical considerations.

In-silico toxicity approaches that use computational tools are considered to be useful for forecasting the toxicity of discovered phytochemicals. In this study, *in-silico* techniques were used to assess the toxicity

of phytochemicals. *In-silico* was used to predict the hERG inhibitor, AMES, hepatotoxicity, carcinogenicity, and skin-irritating qualities of selected compounds. Punarnavoside, the top compound, was found to be free of hERG toxicity, AMES toxicity, skin irritation and hepatotoxicity. The optimal chemical combination with the protein target of 100 ns was simulated using molecular dynamics. MD simulation confirmed the stability and volatility of the drug candidate in relation to the target protein.

The punarnavoside-SGLT2 complex and flavone-SGLT2 complex were validated by interpreting the RMSD, RMSF, and hydrogen bond interactions during simulation to form a stable interaction. The simulation studies indicated that punarnavoside-SGLT2 complex formed a greater number of H-bonds, which may confer rigidity for the complex. In contrast, flavone with SGLT2 complex formed a least number of H-bond pairs, which could affect the stability of the complex.

DFT is the most commonly used and widely applied quantum theory for calculating the electronic structures of atoms and molecules [37]. DFT is used in drug discovery to investigate the specific electronic characteristics of particular drug molecules. It is also used in conjunction with molecular mechanics-based approaches to investigate the drug-receptor interactions. When drug molecules interact with active sites in target proteins, DFT can describe the reaction mechanisms with chemical precision that molecular mechanics cannot match. As a result, DFT is useful for characterizing drug properties as well as how drug inhibit or activate their target molecules. Several research works reported that the test molecules which are having a higher energy gap between HOMO and LUMO when compared to standard drug are known to possess more therapeutic activity [38]. The higher scoring compounds, punarnavoside and flavone, revealed a larger energy band gap in DFT analysis. Punarnavoside and flavone could thus be lead molecules that can be further developed into candidate drugs against CKD after confirmation by *in vitro* and *in vivo* studies.

4. CONCLUSION

Traditional plant extracts and bioactive compounds from plants are used in the prevention of chronic diseases, helping to maintain health, lowering treatment costs, and improving the quality of life. SGLT2 inhibitors are currently the most promising therapeutic options and initiatives being investigated for CKD. The current study looks at a possible therapeutic agent derived from *B. diffusa* to prevent CKD. Among the ten compounds tested, two bioactive compounds, punarnavoside and flavone exhibited a higher binding affinity to the target protein, SGLT2 with values of $-10.2 \text{ kcal} \times \text{mol}^{-1}$ and $-9.3 \text{ kcal} \times \text{mol}^{-1}$, respectively. The pharmacokinetics and physicochemical properties of punarnavoside and flavone indicate that they are non-toxic and drug-like with only minor formulation changes required to improve GI absorption. Molecular dynamics simulation was used to investigate the stability of the ligand-receptor complex, and it was shown that the punarnavoside and SGLT2 complex remain stable throughout the simulation. The stability of the ligand-receptor complexes was investigated using molecular dynamics simulation, and it was discovered that the punarnavoside and SGLT2 complex remain stable throughout the simulation and this may be better than the flavone - SGLT2 complex. The results of the density functionality theory also revealed how stable punarnavoside is in its natural state. In conclusion, the bioactive substance, punarnavoside from *B. diffusa* could serve as a potential lead molecule in offering therapeutic effects against CKD through inhibition of SGLT2. Further research utilizing both *in vitro* and *in vivo* experiments are needed to confirm the ability of punarnavoside as a therapeutic agent for CKD. The density functionality theory results also revealed the natural stability of punarnavoside and flavone. Finally, the bioactive compounds punarnavoside and flavone from *B. diffusa* may serve as potential lead molecules in providing therapeutic effects against CKD via SGLT2 inhibition. More research, including both *in vitro* and *in vivo* experiments, is needed to confirm their efficacy as CKD therapeutic agents.

5. METHODS

5.1 Phytochemicals identification

A total of twenty-five phytochemical compounds from *B. diffusa*, were identified through Indian Medicinal Plants, Phytochemistry, and Therapeutics (IMPPAT) database (<https://cb.imsc.res.in/imppat/home>) [39]. It is a curated database containing information on traditional Indian plants and its related information [40]. The structures of identified phytochemicals and standard drug were drawn by Chemsketch software (ACD/Chemsketch software, v2021.2.2, Toronto, Ontario, Canada) and energy optimized with MMFF94 (Merck molecular force field 94). All the twenty-five selected

phytochemicals, along with the reference CKD drug (Dapaglifozin), were docked against the target protein, SGLT2.

5.2 Protein preparation

Target proteins of CKD were identified through literature and, the Therapeutic Target Database (TTD) [41]. Among these, Sodium/glucose co-transporter 2 (SGLT2) has been chosen as the target for this study. The protein sequence and functional information of SGLT2 were retrieved from UniprotKB database (<https://www.uniprot.org/>) [42]. The protein structure prediction server (Swiss Model server) was used to determine the 3D structure of the target protein from its amino acid sequence [43]. The best model was selected based on GMQE and QMEAND scale of 0 to 1 for overall model quality, with higher numbers indicating greater predicted quality [44]. The selected models were evaluated using the Ramachandran plot (Supplementary Figure 1) and the 3D PDB file was retrieved. Figure 1 shows the 3D structure of SGLT2 modelled using Swiss Model server.

5.3 Active site prediction

PrankWeb (<https://prankweb.cz/>) is a web-based tool that predicts ligand binding sites on the structure of protein. It provides access to P2Rank, a machine-learning approach for predicting ligand binding sites. PrankWeb application allows users to do the prediction and visually evaluate the anticipated binding sites using an integrated sequence-structure view [45]. It offers several pockets and ranks depending on the score and likelihood. Ligand binding site was predicted using this tool for SGLT2 target protein.

5.4 Molecular docking

The PyRx software 0.8 in the AutoDock Vina programme was used to assess the structure-based virtual screening of highly active phytochemicals from *B. diffusa* [46]. For this purpose, Vina wizard tool from PyRx software was used to generate a receptor grid box, once the active binding site based on the potential amino acids was predicted in the target protein. The obtained ligands of *B. diffusa* and dapaglifozin were then docked against SGLT2 protein using PyRx default settings. The docked conformation of the ligands was arranged according to their higher binding affinity (or lower binding energy in kcal \times mol⁻¹) for further evaluation. Further, the BIOVIA Discovery Studio Visualizer v21.1.0.20298 tool was used to evaluate the binding relationship in the protein-ligand complexes.

5.5 Prediction of ADMET and drug-likeness properties

For selected bioactive compounds, the SwissADME online tool (<http://www.swissadme.ch/>) was used to predict their physicochemical parameters (molecular weight, number of rotatable bonds, hydrogen bond acceptor and donor, molar refractivity, solubility, gastrointestinal absorption, blood-brain barrier crossing, Lipinski's rule, bioavailability score, and synthetic accessibility) and ADMET properties (absorption, distribution, metabolism, excretion and toxicity) [47]. The toxicity and carcinogenicity profiles of the phytochemicals were predicted by uploading the canonical SMILES (simplified molecular-input line-entry system) of the chosen phytochemicals to the online pkCSM-pharmacokinetics web server (<http://biosig.unimelb.edu.au/pkcsm/prediction>) [48].

5.6 Molecular dynamics (MD) simulation

MD simulation studies aim to observe the behavior of protein and selected phytochemicals such as, conformational changes, biomolecules binding conformation, and inter molecular interactions between the selected phytochemical with the target protein-ligand complexes (PLC). The MD simulation performed through DESMOND computer package, created by D.E. Shaw's research group was used. The potential consequences of PLC at target binding sites in physiological circumstances are highlighted using MD simulation (Schrödinger, LLC, Schrödinger Release: QikProp). The panel for system developers: Initially, the panel allows us to build a box (10 \times 10 \times 10) that contains water molecules and physiological characteristics like pH. If the pH is not present or if it needs to be raised or decreased to fulfil the specific criteria of the study technique, Na⁺ or Cl⁻ ions may be added. The docked protein-ligand complexes were solved using the straightforward orthorhombic point-charge (SPC) water model. The solvated system was neutralized using counter ions while the physiological salt content was kept at 0.15 M. The PLC system was subjected to the

OPLS AA (Optimal Potentials for Liquid Simulation - All Atom) force field [49]. Minimization: With the aid of the system builder panel, a moderate minimization will be carried out on the ready PLC at approximately 100 ps. In molecular dynamics with two ps relaxation durations, the integrator of the Reversible Reference System Propagator Algorithms (RESPA), the Martyna-Tobias-Klein barostat, and the Nose-Hoover chain thermostat were all used [50, 51]. The equilibrated system was used to produce the last iteration of the MD simulation. The NPT (Isothermal-Isobaric ensemble, constant temperature, constant pressure, and constant number of particles) ensemble with the default relaxation parameters was used to perform the MD simulation for 100 ns at 310.15 K temperature and 1.0 bar pressure [52]. A simulation interaction diagram was used to assess the results once the simulation is completed [33].

5.7 Density functional theory (DFT)

The selected top-scored bioactive compounds were subjected to computer simulations using the Gaussian 03W package and the Gauss View molecular visualization program [53]. The molecular structures of the selected bioactive compounds were optimized using the DFT/Becke-3-Lee-Yang-Parr (B3LYP) approach and a 6-311G (d,p) basis set. The optimized structures were used to compute the frontier molecular orbital energies (lowest unoccupied molecular orbital [E_{LUMO}], highest occupied molecular orbital [E_{HOMO}], and their energy gap [E_g]) of both compounds. Using the molecular visualization application, Gauss View, the generated molecular orbital energy diagrams of the selected bioactive compounds were shown [54].

5.8 Metabolite prediction

The crucial enzyme in phase I metabolism is cytochrome P450. Various cytochrome P450 sites were predicted by SmartCyp (<https://smartcyp.sund.ku.dk/>), and its isoforms such as 2C9, 2D6, 3A4 serve as the prediction models [55]. Rank, Atom (type and number), Score, Energy, Accessibility, 2DSASA, and similarity are the parameters that are displayed as the output. The top three sites of metabolism under 3A4 isoforms were identified for the selected ligand and the structures of the metabolites were drawn using Chemsketch software.

5.9 Metabolite docking

The top three metabolites of Punarnavoside were used to perform molecular docking against the binding pockets of SGLT2 protein using PyRx default settings. The docked conformations of the ligands were arranged according to their binding affinity (lower binding energy in kcal \times mol⁻¹) and, selected for further examination by PyRx. Finally, the BIOVIA Discovery Studio Visualizer v21.1.0.20298, was used to study the binding relationship between the protein-ligand complex.

SUPPLEMENTARY FILE



Supplementary Figure 1. Ramachandran plot for the SGLT2 protein modelled using Swiss Model tool.

Acknowledgements: SJK, SK and KS gratefully acknowledge the Management of Kalasalingam Academy of Research and Education for the research facility. OS thanks All India Council of Technical Education (AICTE) for the GATE post-graduate fellowship.

Author contributions: Concept – S.J.K., S.K., K.S.; Design – S.J.K., S.K., K.S.; Supervision – K.S.; Resources – K.S., P.P.; Materials: S.J.K., S.K., P.P., K.S.; Data Collection and/or Processing – S.J.K., O.S., S.K., K.S.; Analysis and/or Interpretation – S.J.K., S.K., P.P., K.S.; Literature Search – S.J.K., O.S.; Writing – S.J.K., S.K., K.S.; Critical Reviews – S.J.K., O.S., S.K., P.P., K.S..

Conflict of interest statement: The authors report no financial interest that might pose a potential, perceived or real conflict of interest.

REFERENCES

- [1] Levey AS, Coresh J. Chronic kidney disease. *Lancet*. 2012;379(9811):165-180. [https://doi.org/10.1016/S0140-6736\(11\)60178-5](https://doi.org/10.1016/S0140-6736(11)60178-5).
- [2] Levey AS, Atkins R, Coresh J, Cohen EP, Collins AJ, Eckardt KU, Nahas ME, Jaber BL, Jadoul M, Levin A, Powe NR, Rossert J, Wheeler DC, Lameire N, Eknoyan G. Chronic kidney disease as a global public health problem: approaches and initiatives - a position statement from Kidney Disease Improving Global Outcomes. *Kidney Int*. 2007;72(3):247-259. <https://doi.org/10.1038/sj.ki.5002343>.
- [3] Valente MA, Hillege HL, Navis G, Voors AA, Dunselman PH, van Veldhuisen DJ, Damman K. The Chronic Kidney Disease Epidemiology Collaboration equation outperforms the Modification of Diet in Renal Disease equation for estimating glomerular filtration rate in chronic systolic heart failure. *Eur J Heart Fail*. 2014 ;16(1):86-94. <https://doi.org/10.1093/eurjhf/hft128>.
- [4] Webster AC, Nagler EV, Morton RL, Masson P. Chronic Kidney Disease. *Lancet*. 2017;389(10075):1238-1252. [https://doi.org/10.1016/S0140-6736\(16\)32064-5](https://doi.org/10.1016/S0140-6736(16)32064-5).
- [5] Xie Y, Bowe B, Mokdad AH, Xian H, Yan Y, Li T, Maddukuri G, Tsai CY, Floyd T, Al-Aly Z. Analysis of the Global Burden of Disease study highlights the global, regional, and national trends of chronic kidney disease epidemiology from 1990 to 2016. *Kidney Int*. 2018;94(3):567-581. <https://doi.org/10.1016/j.kint.2018.04.011>.
- [6] Dodd R, Palagyi A, Guild L, Jha V, Jan S. The impact of out-of-pocket costs on treatment commencement and adherence in chronic kidney disease: a systematic review. *Health Policy Plan*. 2018;33(9):1047-1054. <https://doi.org/10.1093/heapol/czy081>.
- [7] Basile C, Brandenburg V, Ureña Torres PA. Natural Vitamin D in Chronic Kidney Disease. *Vitamin D in Chronic Kidney Disease*. 2016:465-491. https://doi.org/10.1007/978-3-319-32507-1_28.
- [8] Ogutmen B, Yildirim A, Sever MS, Bozfakioğlu S, Ataman R, Ereğ E, Cetin O, Emel A. Health-related quality of life after kidney transplantation in comparison intermittent hemodialysis, peritoneal dialysis, and normal controls. *Transplant Proc*. 2006;38(2):419-21. <https://doi.org/10.1016/j.transproceed.2006.01.016>.
- [9] Romagnani P, Remuzzi G, Glassock R, Levin A, Jager KJ, Tonelli M, Massy Z, Wanner C, Anders HJ. Chronic kidney disease. *Nat Rev Dis Primers*. 2017;3:17088. <https://doi.org/10.1038/nrdp.2017.88>.
- [10] Jha V. Herbal medicines and chronic kidney disease. *Nephrology (Carlton)*. 2010;15 Suppl 2:10-17. <https://doi.org/10.1111/j.1440-1797.2010.01305.x>.
- [11] Prasathkumar M, Anisha S, Dhriya C, Becky R, Sadhasivam S. Therapeutic and pharmacological efficacy of selective Indian medicinal plants—a review. *Phytomedicine Plus*. 2021;1(2):100029. <https://doi.org/10.1016/j.phyplu.2021.100029>.
- [12] Mishra S, Aeri V, Gaur PK, Jachak SM. Phytochemical, therapeutic, and ethnopharmacological overview for a traditionally important herb: *Boerhavia diffusa* Linn. *BioMed Res Int*. 2014;2014(1):808302. <https://doi.org/10.1155/2014/808302>.
- [13] Khan MU, Basist P, Zahiruddin S, Ibrahim M, Parveen R, Krishnan A, Ahmad S. Nephroprotective potential of *Boerhaavia diffusa* and *Tinospora cordifolia* herbal combination against diclofenac induced nephrotoxicity. *South Afr J Bot*. 2022;151:238-247. <https://doi.org/10.1016/j.sajb.2022.01.038>.
- [14] Gaur PK, Rastogi S, Lata K. Correlation between phytochemicals and pharmacological activities of *Boerhavia diffusa* Linn with traditional-ethnopharmacological insights. *Phytomedicine Plus*. 2022;2(2):100260. <https://doi.org/10.1016/j.phyplu.2022.100260>.
- [15] Patil KS, Bhalsing SR. Ethnomedicinal uses, phytochemistry and pharmacological properties of the genus *Boerhavia*. *J Ethnopharmacol*. 2016;182:200-220. <https://doi.org/10.1016/j.jep.2016.01.042>.
- [16] Oburai NL, Rao VV, Bonath RBN. Comparative clinical evaluation of *Boerhavia diffusa* root extract with standard Enalapril treatment in Canine chronic renal failure. *J Ayurveda and Integr Med*. 2015;6(3):150. <https://doi.org/10.4103/0975-9476.166390>.

- [17] Pareta SK, Patra KC, Mazumder PM, Sasmal D. Aqueous extract of *Boerhaavia diffusa* root ameliorates ethylene glycol-induced hyperoxaluric oxidative stress and renal injury in rat kidney. *Pharm Biol.* 2011;49(12):1224-1233. <https://doi.org/10.3109/13880209.2011.581671>.
- [18] Neumiller JJ, White JR, Campbell RK. Sodium-glucose co-transport inhibitors: progress and therapeutic potential in type 2 diabetes mellitus. *Drugs.* 2010;70:377-385. <https://doi.org/10.2165/11318680-000000000-00000>.
- [19] Yaribeygi H, Butler AE, Atkin SL, Katsiki N, Sahebkar A. Sodium-glucose cotransporter 2 inhibitors and inflammation in chronic kidney disease: Possible molecular pathways. *J Cell Physiol.* 2019;234(1):223-230. <https://doi.org/10.1002/jcp.26851>.
- [20] Winiarska A, Knysak M, Nabrdalik K, Gumprecht J, Stompór T. Inflammation and oxidative stress in diabetic kidney disease: the targets for SGLT2 inhibitors and GLP-1 receptor agonists. *Int J Mol Sci.* 2021;22(19):10822. <https://doi.org/10.3390/ijms221910822>.
- [21] Malathi K, Ramaiah S. Bioinformatics approaches for new drug discovery: a review. *Biotechnol Genet Eng Rev.* 2018;34(2):243-260. <https://doi.org/10.1080/02648725.2018.1502984>.
- [22] Kalimuthu AK, Panneerselvam T, Pavadai P, Pandian SRK, Sundar K, Murugesan S, Ammunje DN, Kumar S, Arunachalam S, Kunjiappan S. Pharmacoinformatics-based investigation of bioactive compounds of Rasam (South Indian recipe) against human cancer. *Sci Rep.* 2021;11(1):21488. <https://doi.org/10.1038/s41598-021-01008-9>.
- [23] Askari H, Sanadgol N, Azarnezhad A, Tajbakhsh A, Rafiei H, Safarpour AR, Gheibihayat SM, Raeis-Abdollahi E, Savardashtaki A, Ghanbariasad A, Omidifar N. Kidney diseases and COVID-19 infection: causes and effect, supportive therapeutics and nutritional perspectives. *Heliyon.* 2021;7(1):e06008. <https://doi.org/10.1016/j.heliyon.2021.e06008>.
- [24] Sinan KI, Akpulat U, Aldahish AA, Celik Altunoglu Y, Baloglu MC, Zheleva-Dimitrova D, Gevrenova R, Lobine D, Mahomoodally MF, Etienne OK, Zengin G, Mahmud S, Capasso R. LC-MS/HRMS Analysis, Anti-Cancer, Anti-Enzymatic and Anti-Oxidant Effects of *Boerhaavia diffusa* Extracts: A Potential Raw Material for Functional Applications. *Antioxidants (Basel).* 2021;10(12):2003. <https://doi.org/10.3390/antiox10122003>.
- [25] Lin X, Li X, Lin X. A review on applications of computational methods in drug screening and design. *Molecules.* 2020;25(6):1375. <https://doi.org/10.3390/molecules25061375>.
- [26] Ahmed S, Islam N, Shahinozzaman M, Fakayode SO, Afrin N, Halim MA. Virtual screening, molecular dynamics, density functional theory and quantitative structure activity relationship studies to design peroxisome proliferator-activated receptor- γ agonists as anti-diabetic drugs. *J Biomol Struct Dyn.* 2021;39(2):728-742. <https://doi.org/10.1080/07391102.2020.1714482>.
- [27] Vora J, Patel S, Sinha S, Sharma S, Srivastava A, Chhabria M, Shrivastava N. Structure based virtual screening, 3D-QSAR, molecular dynamics and ADMET studies for selection of natural inhibitors against structural and non-structural targets of Chikungunya. *J Biomol Struct Dyn.* 2019 ;37(12):3150-3161. <https://doi.org/10.1080/07391102.2018.1509732>.
- [28] DeFronzo RA, Reeves WB, Awad AS. Pathophysiology of diabetic kidney disease: impact of SGLT2 inhibitors. *Nature Rev Nephrol.* 2021;17(5):319-334. <https://doi.org/10.1038/s41581-021-00393-8>.
- [29] Śledź P, Cafilisch A. Protein structure-based drug design: from docking to molecular dynamics. *Curr Opin Struct Biol.* 2018;48:93-102. <https://doi.org/10.1016/j.sbi.2017.10.010>.
- [30] Selby-Pham SN, Miller RB, Howell K, Dunshea F, Bennett LE. Physicochemical properties of dietary phytochemicals can predict their passive absorption in the human small intestine. *Sci Rep.* 2017;7(1):1931. <https://doi.org/10.1038/s41598-017-01888-w>.
- [31] Jia C-Y, Li J-Y, Hao G-F, Yang G-F. A drug-likeness toolbox facilitates ADMET study in drug discovery. *Drug Discov Today.* 2020;25(1):248-258. <https://doi.org/10.1016/j.drudis.2019.10.014>.
- [32] Chen X, Li H, Tian L, Li Q, Luo J, Zhang Y. Analysis of the physicochemical properties of acaricides based on Lipinski's rule of five. *J Comput Biol.* 2020;27(9):1397-1406. <https://doi.org/10.1089/cmb.2019.0323>.
- [33] Palanichamy C, Pavadai P, Panneerselvam T, Arunachalam S, Babkiewicz E, Ram Kumar Pandian S, Shanmugampillai Jeyarajaguru K, Nayak Ammunje D, Kannan S, Chandrasekaran J, Sundar K, Maszczyk P, Kunjiappan S. Aphrodisiac Performance of Bioactive Compounds from *Mimosa pudica* Linn.: In Silico Molecular Docking and Dynamics Simulation Approach. *Molecules.* 2022;27(12):3799. <https://doi.org/10.3390/molecules27123799>.
- [34] Tsopelas F, Tsagkrasouli M, Poursanidis P, Pitsaki M, Vasios G, Daniais P, Panderi I, Tsantili-Kakoulidou A, Giaginis C. Retention behavior of flavonoids on immobilized artificial membrane chromatography and correlation with cell-based permeability. *Biomed Chromatogr.* 2018;32(3). <https://doi.org/10.1002/bmc.4108>.
- [35] Rathaur P, S R JK. Metabolism and Pharmacokinetics of Phytochemicals in the Human Body. *Curr Drug Metab.* 2019;20(14):1085-1102. <https://doi.org/10.2174/1389200221666200103090757>.
- [36] Ahmad I, Khan H, Serdaroglu G. Physicochemical properties, drug likeness, ADMET, DFT studies, and in vitro antioxidant activity of oxindole derivatives. *Comput Biol Chem.* 2023;104:107861. <https://doi.org/10.1016/j.compbiolchem.2023.107861>.
- [37] Adekoya OC, Adekoya GJ, Sadiku ER, Hamam Y, Ray SS. Application of DFT calculations in designing polymer-based drug delivery systems: An overview. *Pharmaceutics.* 2022;14(9):1972. <https://doi.org/10.3390/pharmaceutics14091972>.

- [38] Akash S, Aovi FI, Azad MAK, Kumer A, Chakma U, Islam MR, Mukerjee N, Rahman MM, Bayil I, Rashid S, Sharma R. A drug design strategy based on molecular docking and molecular dynamics simulations applied to development of inhibitor against triple-negative breast cancer by Scutellarein derivatives. *Plos One*. 2023;18(10):e0283271. <https://doi.org/10.1371/journal.pone.0283271>.
- [39] Kim S, Chen J, Cheng T, Gindulyte A, He J, He S, Li Q, Shoemaker BA, Thiessen PA, Yu B, Zaslavsky L, Zhang J, Bolton EE. PubChem in 2021: new data content and improved web interfaces. *Nucleic Acids Res*. 2021;49(D1):D1388-D1395. <https://doi.org/10.1093/nar/gkaa971>.
- [40] Mohanraj K, Karthikeyan BS, Vivek-Ananth RP, Chand RPB, Aparna SR, Mangalapandi P, Samal A. IMPPAT: A curated database of Indian Medicinal Plants, Phytochemistry And Therapeutics. *Sci Rep*. 2018;8(1):4329. <https://doi.org/10.1038/s41598-018-22631-z>.
- [41] Zhou Y, Zhang Y, Lian X, Li F, Wang C, Zhu F, Qiu Y, Chen Y. Therapeutic target database update 2022: facilitating drug discovery with enriched comparative data of targeted agents. *Nucleic Acids Res*. 2022 Jan 7;50(D1):D1398-D1407. <https://doi.org/10.1093/nar/gkab953>.
- [42] Luebbert L, Pachter L. Efficient querying of genomic reference databases with gget. *Bioinformatics*. 2023;39(1):btac836. <https://doi.org/10.1093/bioinformatics/btac836>.
- [43] Waterhouse A, Bertoni M, Bienert S, Studer G, Tauriello G, Gumienny R, Heer FT, de Beer TAP, Rempfer C, Bordoli L, Lepore R, Schwede T. SWISS-MODEL: homology modelling of protein structures and complexes. *Nucleic Acids Res*. 2018;46(W1):W296-W303. <https://doi.org/10.1093/nar/gky427>.
- [44] Studer G, Rempfer C, Waterhouse AM, Gumienny R, Haas J, Schwede T. QMEANDisCo – distance constraints applied on model quality estimation. *Bioinformatics*. 2020;36(6):1765-1771. <https://doi.org/10.1093/bioinformatics/btz828>.
- [45] Jendele L, Krivak R, Skoda P, Novotny M, Hoksza D. PrankWeb: a web server for ligand binding site prediction and visualization. *Nucleic Acids Res*. 2019;47(W1):W345-W349. <https://doi.org/10.1093/nar/gkz424>.
- [46] Dallakyan S, Olson AJ. Small-molecule library screening by docking with PyRx. *Methods Mol Biol*. 2015;1263:243-250. https://doi.org/10.1007/978-1-4939-2269-7_19.
- [47] DeLano WL. Pymol: An open-source molecular graphics tool. *CCP4 Newsl Protein Crystallogr*. 2002;40(1):82-92.
- [48] Lohohola PO, Mbala BM, Bambi S-MN, Mawete DT, Matondo A, Mvondo JGM. In silico ADME/T properties of quinine derivatives using SwissADME and pkCSM webservers. *Int J Trop Dis Health*. 2021;42(11):1-12. <https://doi.org/10.9734/ijtdh/2021/v42i1130492>.
- [49] Jorgensen WL, Maxwell DS, Tirado-Rives J. Development and testing of the OPLS all-atom force field on conformational energetics and properties of organic liquids. *J Am Chem Soc*. 1996;118(45):11225-11236. <https://doi.org/10.1021/ja9621760>.
- [50] Martyna GJ, Klein ML, Tuckerman M. Nosé-Hoover chains: The canonical ensemble via continuous dynamics. *J Chem Phys*. 1992;97(4):2635-2643. <https://doi.org/10.1063/1.463940>.
- [51] Cheng A, Merz KM. Application of the Nosé-Hoover chain algorithm to the study of protein dynamics. *J Phys Chem*. 1996;100(5):1927-1937. <https://doi.org/10.1021/jp951968y>.
- [52] Kalibaeva G, Ferrario M, Ciccotti G. Constant pressure-constant temperature molecular dynamics: A correct constrained NPT ensemble using the molecular virial. *Mol Phys*. 2003;101(6):765-778. <https://doi.org/10.1080/0026897021000044025>.
- [53] Sánchez-Bojorge NA, Rodríguez-Valdez LM, Flores-Holguín N. DFT calculation of the electronic properties of fluorene-1, 3, 4-thiadiazole oligomers. *J Mol Model*. 2013;19:3537-3542. <https://doi.org/10.3390/molecules27123799>.
- [54] Parasuraman P, Alagarsamy V, Udayakumar P, Soundararajan M, Joshi SD, Ramalingam S, Ammunje DN. Graph theoretical analysis, in silico modeling, prediction of toxicity, metabolism and synthesis of novel 2-(methyl/phenyl)-3-(4-(5-substituted-1,3,4-oxadiazol-2-yl) phenyl) quinazolin-4(3H)-ones as NMDA receptor inhibitor. *Drug Dev Res*. 2019;80(3):368-385. <https://doi.org/10.1002/ddr.21511>.
- [55] Rydberg P, Gloriam DE, Olsen L. The SMARTCyp cytochrome P450 metabolism prediction server. *Bioinformatics*. 2010;26(23):2988-2989. <https://doi.org/10.1093/bioinformatics/btq584>.